Original paper

Bismuth and bismuth–antimony sulphosalts from Kutná Hora vein Ag–Pb–Zn ore district, Czech Republic

Richard PAŽOUT [1]*, Jiří SEJKORA[2], Vladimír ŠREIN[3]

[1] *Institute of Chemical Technology, Technická 5, 166 28 Prague 6, Czech Republic; richard.pazout@vscht.cz*
[2] *Department of Mineralogy and Petrology, National Museum, Cirkusová 1740, 193 00 Prague 9, Czech Republic*
[3] *Czech Geological Survey, Klárov 3, 118 21 Prague 1, Czech Republic*
**Corresponding author*

A new, previously unknown association of Pb–Bi–Sb–Ag sulphosalt minerals has been found in samples from mine dumps of the Staročeské pásmo Lode of the Kutná Hora Ag–Pb–Zn ore district, central Bohemia, Czech Republic. These minerals form polymineral aggregates up to 1–3 cm in quartz or base sulphides. Apart from numerous members of lillianite homologous series, new occurrences of aramayoite, bismuthinite, cosalite, ikunolite, izoklakeite, matildite, galena$_{ss}$, Bi-rich jamesonite, Bi-rich boulangerite, Bi-rich owyheeite and Bi-rich semseyite have been identified. An extraordinary extent of the Bi–Sb substitution is characteristic of the studied association. Bi-rich mineralization of this scope has not been previously known from the Kutná Hora ore district.

The origin of this sulphosalt mineralization is related to the penetration of lower temperature fluids (*c.* 100–250 °C) into tectonically opened fractures in older ore veins filling. Virtually no mobilization of elements from the earlier vein filling took place; hydrothermal fluids must have been relatively rich in Ag and Pb and simultaneously poor in Cu. High Bi content was characteristic of the initial stage of the mineralization. Gradually, the Bi/Sb ratio decreased considerably with more Sb-rich minerals originating. At the final stage, Bi-rich Pb–Sb sulphosalts with lower Ag contents crystallized.

Keywords: Bi and Bi–Sb sulphosalts, izoklakeite, cosalite, aramayoite, Bi-bearing Pb–Sb sulphosalts, Kutná Hora
Received: 8 June, 2016; accepted: 1 March, 2017; handling editor: F. Laufek
The online version of this article (doi: 10.3190/jgeosci.230) contains supplementary electronic material.

1. Introduction

In the late 1990's, a new, hitherto unknown Bi-mineralization was discovered in the Kutná Hora ore district (60 km east of Prague, Czech Republic), which – unlike other Ag mineralizations found in this district that were associated with antimony – was characterized by the presence of bismuth. An intense search followed and several hundred samples with this mineralization have been found so far.

Interestingly, most of the bismuth and antimony sulphosalts found during the investigation and described here exhibit substantial Sb for Bi substitution. Although Bi–Sb sulphosalts have been described in nature, they are much rarer than either pure Sb- or Bi-sulphosalts. The number of localities worldwide with sulphosalts displaying significant amounts of Bi and Sb simultaneously is very limited (Cook 1997).

Natural sulphosalts that contain both Bi and Sb can be divided into three groups:

a) Bi–Sb sulphosalts containing both Bi and Sb as essential constituents

(i) The kobellite homologous series. Minerals of the tintinaite–kobellite series are the most frequent, while those of the izoklakeite–giessenite series (Moëlo et al. 1995, 2008) are considerably rarer.

(ii) The meneghinite homologous series includes jaskolskiite (Moëlo et al. 1995, 2008).

(iii) The lillianite homologous series with terrywallaceite (Yang et al. 2013), oscarkempffite (Topa et al. 2011) and clino-oscarkempffite (Topa et al. 2013).

(iv) The bismuthinite Bi_2S_3 – stibnite Sb_2S_3 solid solution with intermediate members, the so-called "horobetsuite" (Ghosal and Sack 1999; Sejkora 2002).

v) Garavellite $FeSbBiS_4$ and members of solid solution to berthierite $FeSb_2S_4$ (Bindi and Menchetti 2005).

(vi) Aramayoite $Ag_3Sb_2(Bi, Sb)S_6$ and members of solid solution to baumstarkite $Ag_3Sb_3S_6$ (Effenberger et al. 2002; Kitakaze et al. 2012).

b) Sb sulphosalts with significantly increased Bi content include Bi-rich varieties of jamesonite, boulangerite, bournonite, owyheeite, zinkenite, chalcostibite, robinsonite, meneghinite and other Pb–Sb sulphosalts, whose list and references were given in Cook (1997). An important part of this group are Bi-rich members of the andorite branch of the lillianite homologous series (Pažout 2017).

c) Bi sulphosalts with significantly increased Sb content are represented by Sb-bearing members of the lillianite branch of the lillianite homologous series: Sb-rich varieties of gustavite, vikingite, treasurite, eskimoite and erzwiesite (Pažout 2017).

This paper documents a rare Bi–Sb mineralization from the Staročeské pásmo Lode of the Kutná Hora ore district. It focuses on the characterization of all other bismuth–antimony sulphosalts found and discusses probable conditions of the studied mineralization origin.

2. Geological setting

The Kutná Hora Ag–Pb–Zn ore district (60 km east of Prague, Central Bohemia, Czech Republic) represents a hydrothermal vein type mineralization of Variscan age (Holub et al. 1982). A full list of minerals of the Kutná Hora ore district is given in Malec and Pauliš (1997) and Pauliš (1998).

In general, two mineral assemblages are present in the ore district (Fig. 1), one "silver-rich" in the south, the other "pyrite-rich" in the north (Malec and Pauliš 1997). The silver-rich assemblage consists mainly of miargyrite, pyrargyrite, freibergite, native silver, galena, pyrite, sphalerite, berthierite and Pb–Sb (–Ag) sulphosalts (boulangerite, jamesonite and owyheeite) in quartz–kutnohorite gangue. The pyrite-rich assemblage comprises pyrite, arsenopyrite, sphalerite, Ag-bearing galena, pyrrhotite, marcasite, chalcopyrite, stannite, freibergite–tetrahedrite and Pb–Sb (–Ag) sulphosalts in quartz gangue without kutnohorite. Typical of the latter is the presence of Bi and Sn (each from a different mineralization stage), completely absent in the former, silver-rich assemblage. The pyrite-rich assemblage yields a suite of Pb–Bi–Sb–Ag sulphosalts, many of which are unknown elsewhere in the Czech Republic.

Although several microscopic Bi minerals have been detected before, native Bi (Novák 1964), matildite-like phase (Hoffman and Trdlička 1979) or gustavite (Hoffman et al. 1989), this paper is the first that reports and chemically documents the occurrence of several groups of complex Bi and Bi–Sb sulphosalts from this ore district.

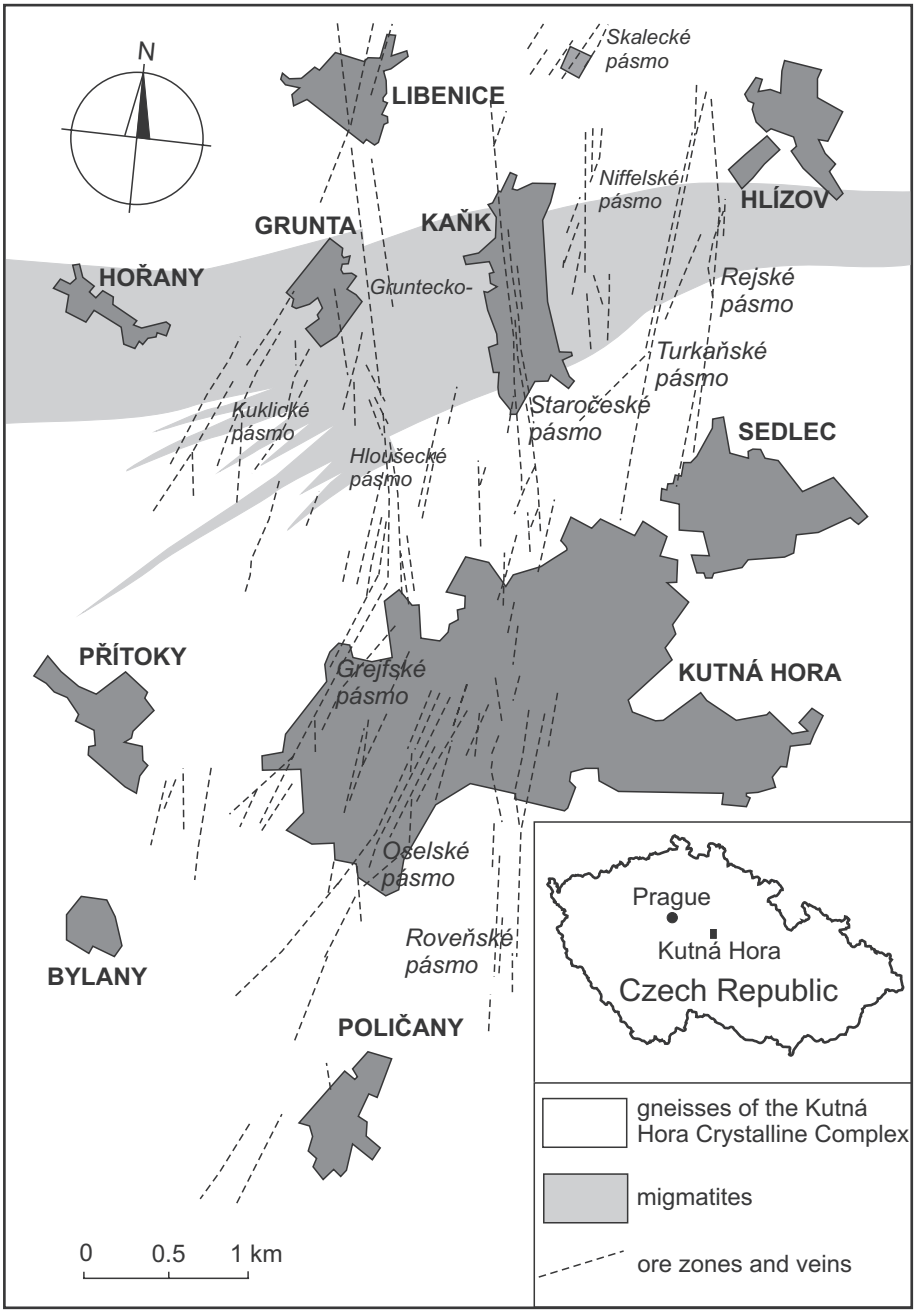

Fig. 1 Map of Kutná Hora ore district. with major ore zones (lodes), after Malec and Pauliš (1997). Each lode ("pásmo" in Czech) consists of several veins.

3. Analytical techniques

Collected samples were viewed under optical microscope, suitable grains were extracted and submitted for X-ray powder diffraction pre-identification to check the presence of Bi sul-

phosalts. The resulting patterns revealed in most cases the presence of a complex mixture of several sulphosalt phases. Silicon holders with the examined bulk powdered samples were then analyzed by X-ray fluorescence spectrometry which showed the presence of Ag, Pb, Bi, Sb and S. Samples which were positively screened for the presence of Bi-sulphosalts were prepared into polished sections.

3.1. Mineral chemistry

More than 150 polished sections, prepared from a representative number of ore specimens collected during field work in 1999–2015, were investigated microscopically and subsequently analysed by electron microprobe at the University of Salzburg. Quantitative chemical analysis was performed with a JEOL JXA-8600 electron microprobe (EMP) in the wave-length dispersive mode (WDS), controlled by a LINK*eXL* system, operated at 25 kV, 35 nA, and 20 s counting time for peaks and 7 s for background, and a beam diameter of 5 µm. The following standards and X-ray lines were used: $CuFeS_2$ (CuK_α, FeK_α), Ag (AgL_α), PbS (PbL_α), Bi_2S_3 (BiL_α, SK_α), Sb_2S_3 (SbL_α), CdTe (CdL_β, TeL_α), Bi_2Te_2S (BiL_α, TeL_α), Bi_2Se_3 (SeK_α). Raw data were corrected with an online ZAF-4 procedure.

A second large portion of polished sections with Bi-sulphosalts was measured on Cameca SX 100 WDS electron microprobe at the National Museum, Prague. The following conditions were employed: accelerating voltage of 25 kV, beam current of 20 nA and electron-beam diameter of 2 µm. The following standards and X-ray lines were used: chalcopyrite (SK_α, CuK_α), Bi (BiL_α), PbS (PbM_α), Ag (AgL_α), halite (ClK_α), Sb_2S_3 (SbL_α), CdTe (CdL_α), pyrite (FeK_α), ZnS (ZnK_α), NiAs (AsL_β), Mn (MnK_α), Sn (SnL_α), InAs (InL_α) and PbSe (SeL_β). Measured data were corrected using PAP software (Pouchou and Pichoir 1985).

Several samples were measured on Cameca SX 100 WDS electron microprobe at the Geological Institute, Czech Academy of Sciences, Prague, and in Bratislava with the same operating conditions. The comparison of results from all used instruments showed a good agreement.

Results of chemical analyses are presented in tables and averaged. Only those with sums between 98 and 102 wt. % were considered and included (unless stated otherwise). Standard deviations for major elements are in the range of 0.X % relative (usually 0.3–0.5 % for Bi, Pb, Sb and Ag); minor elements (Fe, Cu, Cd, Se) are around 0.0X %.

3.2. X-ray powder diffraction

X-ray powder diffraction (PXRD) data were collected on the X'Pert PRO Panalytical diffractometer, step-scanning 0.02°/30 s, radiation CuK_α, 40 kV, 30 mA, angular range 3.3–55° 2θ, point detector with secondary graphite monochromator (Institute of Chemical Technology, Prague). A very small amount of the sample was placed on the surface of a silicon sample holder. Quartz (if contained) in the analyzed sample was used as an internal standard to check the possible displacement. The obtained powder pattern was processed using X-ray powder diffraction software HighScore Plus (Degen et al. 2014) which found angular positions and intensities of reflections. The refinement of unit cell parameters was carried out by least-squares method implemented in the program Firestar-2 (Fergusson et al. 1987); extrapolation function used was $\cos\theta \times \cot\theta + \cot^2\theta$.

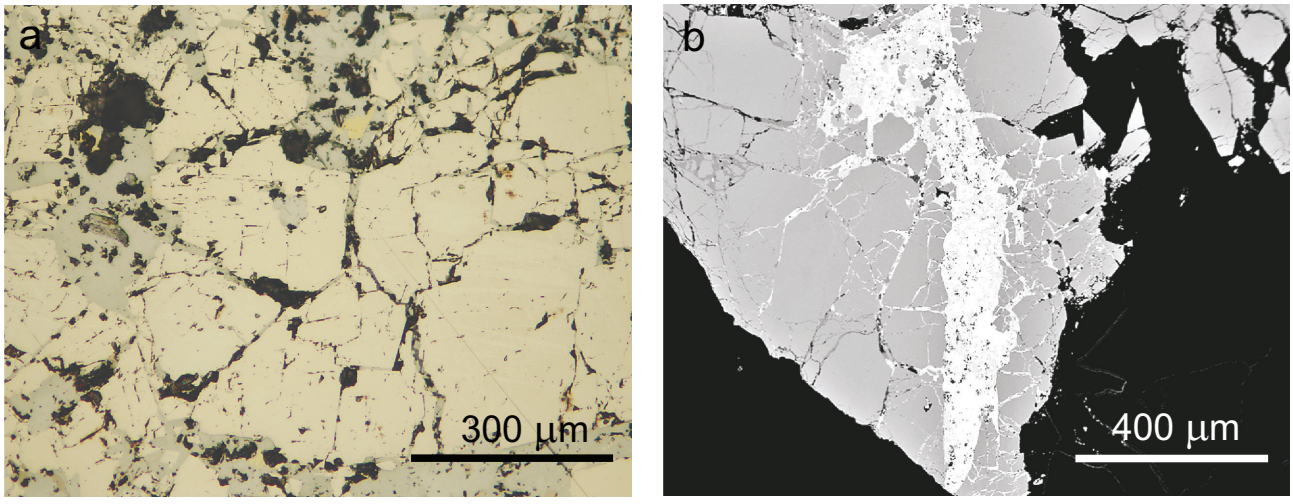

Fig. 2a – Aggregates of izoklakeite (grey) cement earlier (older) tectonically broken grains of pyrrhotite (yellowish); photo in reflected light (one polar); **b -** Aggregates of galena, native Bi, matildite and Bi-sulphosalts (lighter) cementing arsenopyrite breccia (dark grey) or filling fissures therein, BSE image.

4. The Bi and Bi–Sb sulphosalts and their chemical and structural properties

The aggregates of complex Bi sulphosalts occasionally occur in white coarse-grained quartz gangue without any other sulphides. More frequent is their occurrence in quartz gangue with massive or disseminated pyrrhotite, arsenopyrite, stannite, pyrite and other sulphides (Fe-rich sphalerite, galena, marcasite, chalcopyrite or tetrahedrite). Sulphosalt aggregates usually cement earlier, tectonically broken sulphides or fill in fissures in them (Fig. 2a–b). It is clear that their deposition from considerably later fluids was separated from earlier base metal sulphides by a distinct tectonic event. The maximum observed size of aggregates of the studied sulphosalts is 30 × 10 mm. Usually, much of the sulphosalt aggregates is represented by minerals of lillianite homologous series (Pažout 2017).

All studied samples were found in the material from medieval mine dumps of Staročeské pásmo Lode (Old Bohemian Lode) collected in 1999–2015, therefore no information is known about their exact provenance with regard to individual vein structures. Only several samples come from the exploration mining activity in the 1960's. The Staročeské pásmo Lode is the biggest lode of the Kutná Hora ore district, both in terms of the amount of extracted ore and the amount of extracted silver (about 300 tons of Ag). This lode was mined from the discovery

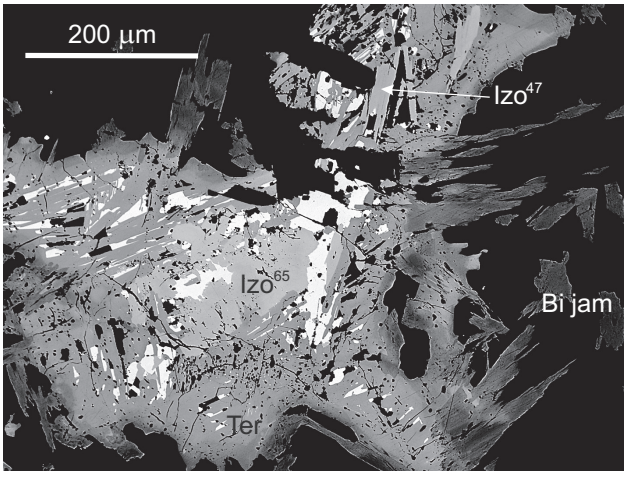

Fig. 3 Backscattered electron image of sample ST 54A. Izo^{65} – Bi-rich izoklakeite (light grey) with Bi/(Sb + Bi) = 0.65, Izo^{47} – Sb-rich izoklakeite with Bi/(Sb + Bi) = 0.47; Bi jam – Bi-rich jamesonite, Ter – terrywallaceite. Galena is white. Lamella-like shapes of Sb-rich izoklakeite Izo^{47} (darker shade of grey than grain marked Izo^{65}) contrast with the corroded shape of the Bi-rich izoklakeite Izo^{65}. The upper index marks the Bi:Sb ratio expressed as Bi/(Sb + Bi) × 100 in at. %.

Tab. 1 Chemical composition of izoklakeite from Kutná Hora (wt. % and formula coefficients based on 105 *apfu*)

	ST 78r	ST 123 J	ST 4 F	ST 54A	ST 81 B2	ST 4 F	ST 78c	ST 4 F	ST 164 B2	ST 81A	ST 114	ST 54 A	ST 4 F
n	2	7	4	1	6	9	1	15	3	3	4	5	2
Pb	44.88	46.04	44.79	42.58	40.03	44.03	43.70	43.14	42.26	42.07	44.81	43.37	43.56
Ag	2.26	2.21	2.03	2.59	3.61	2.24	2.54	2.27	2.33	2.68	1.76	2.08	1.94
Cu	1.02	0.92	1.09	1.04	1.10	0.98	0.96	0.93	0.98	0.87	0.79	0.85	0.86
Fe	0.24	0.19	0.21	0.22	0.20	0.43	0.20	0.23	0.12	0.21	0.24	0.25	0.21
Cd	0.00	0.00	0.00	0.00	0.05	0.01	0.00	0.93	0.00	0.00	0.02	0.00	0.00
Sb	15.16	14.73	14.45	14.23	13.61	12.82	11.91	10.03	9.72	9.94	8.87	8.60	7.52
Bi	18.12	18.17	19.79	21.83	23.72	22.59	23.82	26.25	27.00	27.52	25.95	28.00	29.17
S	17.74	17.94	17.52	18.06	17.53	17.50	17.74	17.28	17.16	17.46	17.06	17.17	17.03
Se	0.05	0.00	0.02	0.08	0.06	0.01	0.07	0.01	0.06	0.06	0.04	0.07	0.00
Total	99.47	100.20	99.94	100.63	99.90	100.66	100.94	100.19	99.64	100.81	99.56	100.38	100.34
Pb	22.24	22.69	22.32	20.84	19.87	21.96	21.73	21.96	21.67	21.24	23.19	22.26	22.56
Ag	2.15	2.09	1.95	2.44	3.44	2.14	2.42	2.22	2.30	2.60	1.75	2.05	1.93
Cu	1.65	1.48	1.77	1.66	1.77	1.59	1.55	1.54	1.64	1.44	1.34	1.42	1.45
Fe	0.43	0.34	0.38	0.40	0.37	0.79	0.37	0.43	0.23	0.39	0.47	0.47	0.40
Cd	0.00	0.00	0.00	0.00	0.04	0.00	0.00	0.00	0.00	0.00	0.02	0.00	0.00
Sb	12.78	12.35	12.25	11.85	11.50	10.88	10.08	8.68	8.48	8.54	7.81	7.51	6.62
Bi	8.90	8.88	9.79	10.60	11.68	11.17	11.75	13.25	13.73	13.77	13.32	14.25	14.98
S	56.78	57.16	56.45	57.11	56.24	56.38	57.01	56.85	56.87	56.94	57.04	56.94	56.98
Se	0.06	0.00	0.03	0.11	0.08	0.01	0.09	0.01	0.08	0.08	0.05	0.10	0.00
N	4.03	4.23	3.86	3.78	4.07	3.78	4.09	4.12	3.96	3.96	4.07	3.92	3.97
Bi/(B + Sb)	0.41	0.42	0.44	0.47	0.50	0.51	0.54	0.60	0.62	0.62	0.63	0.65	0.69
Pb + 2Ag	26.53	26.87	26.22	25.72	26.76	26.24	26.58	26.40	26.26	26.43	26.70	26.35	26.43
Cu + Fe	2.08	1.82	2.16	2.06	2.14	2.38	1.93	1.97	1.88	1.83	1.81	1.90	1.86
Bi + Sb	21.69	21.23	22.4	22.45	23.18	22.5	21.82	21.93	22.21	22.32	21.13	21.76	21.60

n – number of point analyses

N – the width of SnS-like rods in the structure of izoklakeite, i.e. the number of (Sb,Bi) co-ordination pyramids in the rod (Zakrzewski and Makovicky 1986)

and opening of the ore district in the second half of the 13th century until the end of large-scale mining in the first half of 17th century.

4.1. Izoklakeite–giessenite series

Minerals of this series are generally rare Bi–Sb sulphosalts containing minor but essential Cu or Fe and belonging to the kobellite homologous series. Individual members of the kobellite–tintinaite solid solution series can be unambiguously distinguished by means of a calculated *N* value (Zakrzewski and Makovicky 1986). The crystal structure of izoklakeite consists of two types of rods. The larger type of rod is based on a PbS-like archetype, the smaller one represents a SnS-like structure. The parameter *N* expresses the width of the smaller, SnS-like rods, i.e. the number of (Sb,Bi) co-ordination pyramids in the rod. This value is around 2 for kobellite–tintinaite series or 4 for izoklakeite–giessenite series. Moëlo et al. (1995) established for the latter series a simplified formula $Cu_2Pb_{22}Ag_2(Bi,Sb)_{22}S_{57}$; compositional ranges for natural members of this series are the following (*apfu*): Cu + Fe < 2 (means 1.81–2.14), Pb + 2Ag ~ 26 (25.72–27.67), Bi + Sb ~ 22 (20.90–23.18). Since the symmetry of giessenite (Bi-rich) is monoclinic (Makovicky and Karup-Møller 1986) and that of izoklakeite (Sb-rich) is orthorhombic (Armbruster and Hummel 1987), there is apparently only a quasi-continuous solid solution (Moëlo et al. 2008). The exact Sb/Bi ratio at which the symmetry changes is unknown. According to Moëlo et al. (1995), the name izoklakeite is applied to all samples with Sb/Bi atomic ratio close to 1 (i.e. Bi/(Bi + Sb) close to 0.50), even for samples with Bi > Sb. The Bi-richest izoklakeite found so far was identified from Otome mine (Ozawa et al. 1998) with Bi/(Sb + Bi) ratio of 0.68, whereas the

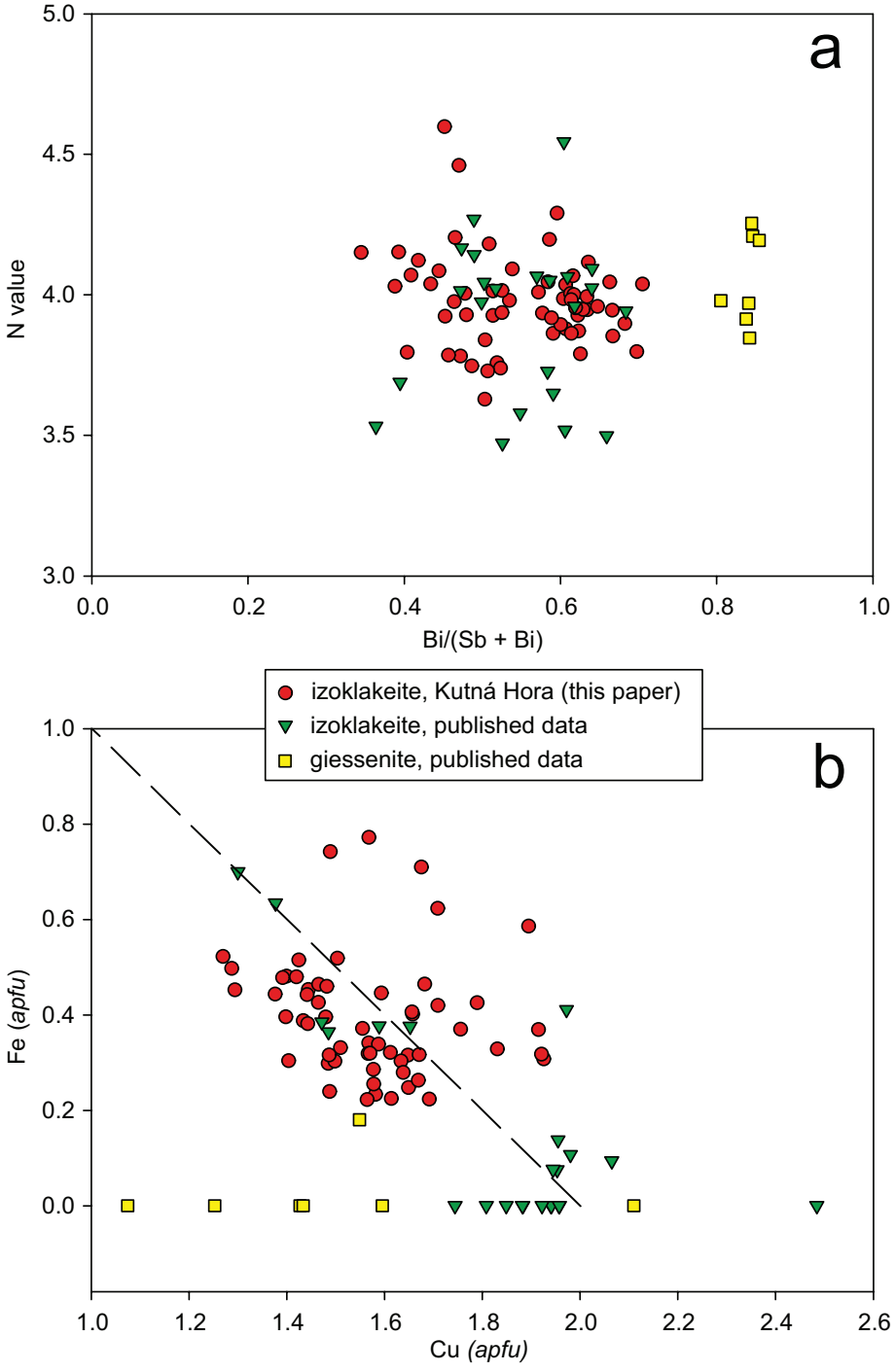

Fig. 4 Substitution diagrams for members of the izoklakeite–giessenite series (*apfu*): **a** – Bi/(Sb + Bi) vs. *N* value; **b** – Cu vs. Fe plot; line indicates ideal content Fe + Cu = 2; Published data for izoklakeite are from Armbruster and Hummel (1987), Harris et al. (1986), Zakrzewski and Makovicky (1986), Moëlo et al. (1995), Ozawa et al. (1998), Orlandi et al. (2010) and Zhang et al. (2015); for giessenite from Karup-Møller (1973), Graeser and Harris (1986), and Makovicky and Karup-Møller (1986).

Bi-poorest (i.e. Sb-richest) giessenite from Giessen (Graeser and Harris 1986) has this ratio equal to 0.81.

In the Kutná Hora ore district, members of izoklakeite–giessenite series usually form lath-shaped or allotriomorphic grains up to 300 μm associated with lillianite homologues, Bi-rich jamesonite and galena (Fig. 3). Izoklakeite replaces earlier PbS_{ss} and is partly replaced by later Sb-rich gustavite, terrywallaceite and the youngest Bi-jamesonite (zoned, with 4–16 wt. % of Bi).

Chemical analyses of izoklakeite from Kutná Hora and their structural formulae are given in Tab. 1. Determined Bi/(Sb + Bi) ratios show a strong variation (0.34–0.70), a range slightly wider than mentioned for izoklakeite so far (Fig. 4a). Thus it is clear that the symmetry change (izoklakeite/giessenite) takes place somewhere in the range of Bi/(Sb + Bi) values of 0.70–0.80. In accordance with the trend observed with other Bi and Bi–Sb sulphosalts from Kutná Hora, the cores of the izoklakeite aggregates are Bi-rich and the rims are Sb-rich. The opposite trend was observed at Altenberg, Austria, where chemically zoned crystals of this series have Sb-rich cores and Bi-rich rims (Putz et al. 2003).

All studied samples have been found to have regular minor contents of Cu and Fe (Fig. 4b), close to ideal Cu + Fe = 2 *apfu*. The two elements occupy a specific site in the izoklakeite crystal structure (Armbruster and Hummel 1987) and are essential for its stabilization. All studied samples of izoklakeite are also characterised by increased contents of Ag (1.59–3.82 wt. %) which do not correlate with either Bi + Sb or Cu + Fe. Silver contents in izoklakeite from Kutná Hora (up to 3.65 *apfu*) are considerably higher (Fig. 5a) than so far established in this mineral (1.95 *apfu*, Harris et al. 1986; 2.19 *apfu*, Moëlo et al. 1995). The Pb vs. Ag graph (Fig. 5b) demonstrates the negative correlation corresponding to the classic substitution in sulphosalts or galena: Ag + (Bi,Sb)→2Pb. The determination of the crystal structure of izoklakeite showed that there is no specific Ag site which confirms that all Ag content in

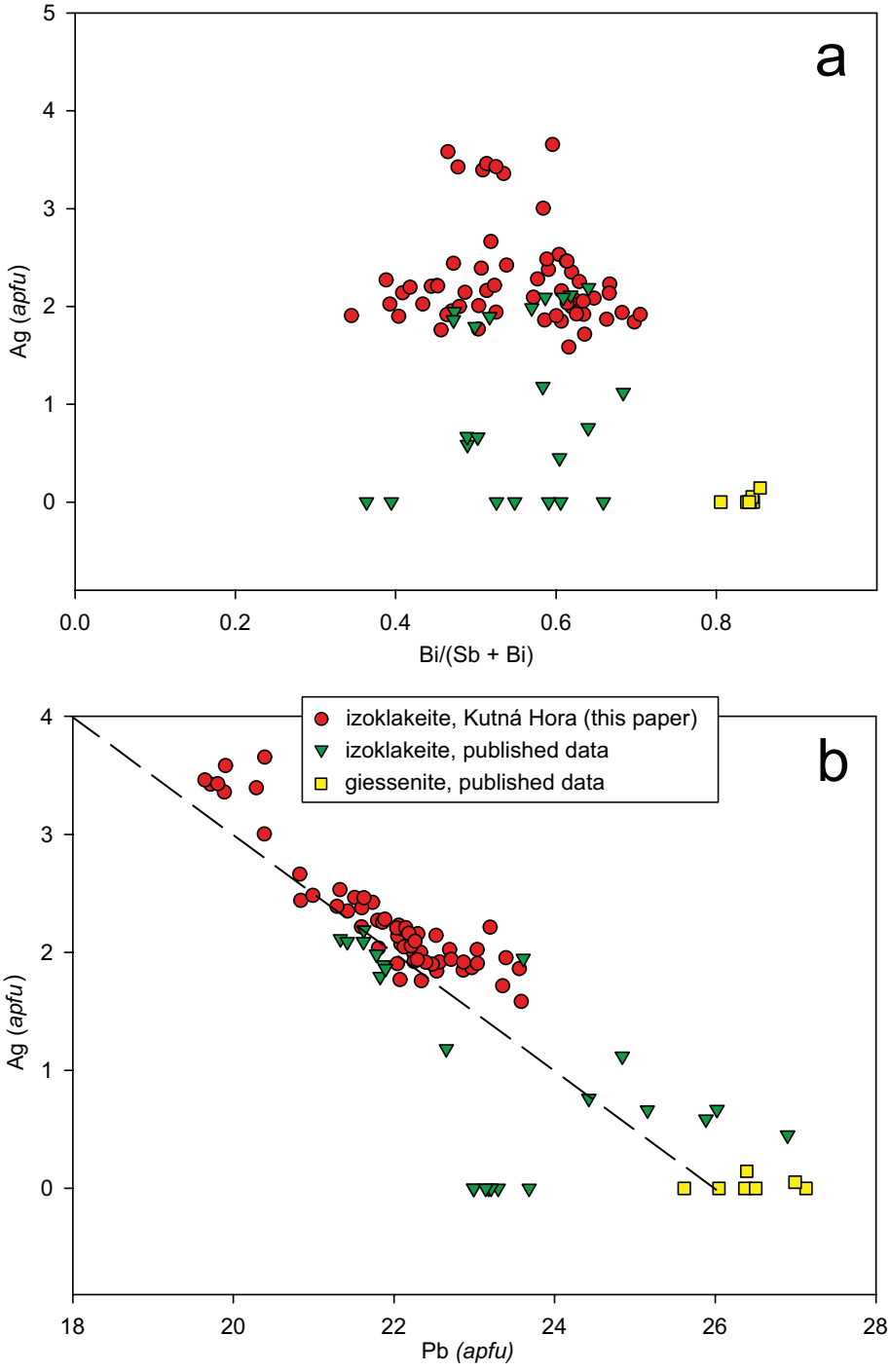

Fig. 5 Substitution diagrams for members of the izoklakeite–giessenite series (*apfu*): **a** – Bi/(Sb + Bi) vs. Ag plot; **b** – Pb vs. Ag plot; line indicates ideal 2Ag – Pb correlation. For sources of the published izoklakeite data, see caption to Fig. 4.

Tab. 2 Unit cell parameters of izoklakeite for monoclinic space group *Pnnm*

		a [Å]	*b* [Å]	*c* [Å]	V [Å^3]	Bi/(Bi + Sb)
Kutná Hora, ST 54A (PXRD)	this paper	34.24(3)	37.95(4)	4.070(4)	5288.1	0.65
Otome mine (PXRD)	Ozawa et al. (1998)	34.067(5)	38.085(4)	4.056(1)	5262.4	0.68
Otome mine (SXRD)	Ozawa et al. (1998)	34.10(1)	38.09(2)	4.060(3)	5273.4	0.68
Seravezza (PXRD)	Orlandi et al. (2010)	34.272(4)	38.351(5)	4.098(1)	5386.2	0.64
Zervreila (SXRD)	Armbruster and Hummel (1987)	34.221(8)	37.933(8)	4.063(3)	5274.2	0.61
Vena (PXRD)	Zakrzewski and Makovicky (1986)	34.07(1)	37.98(1)	4.072(1)	5269.1	0.49

PXRD and SXRD – powder and single-crystal X-ray diffraction, respectively

izoklakeite is a result of the above substitution (Armbruster and Hummel 1987).

Izoklakeite was confirmed by the powder pattern of one of the samples (ST 54A) and unit cell parameters refined for the space group *Pnnm* of Bi-rich izoklakeite (Armbruster and Hummel 1987) are compared in the Tab. 2 with published data of this mineral phase.

4.2. Cosalite

Cosalite occurs in quartz gangue in association with gustavite, terrywallaceite and other lillianite homologues with N > 4 (vikingite, treasurite, eskimoite), native bismuth and galena as lath-shaped or allotriomorphic grains up to 200 μm (Fig. 6). It is marked by a lighter shade of grey in BSE images compared to gustavite, but it is not distinguishable from lillianite homologues with N > 4 or minerals of izoklakeite–giessenite series. The sequence of crystallization and Sb-enrichment trends (younger phases are Sb-richer) are similar to izoklakeite: galena$_{ss}$ → cosalite → Sb-rich gustavite.

The chemical composition of studied cosalite (Tab. 3) is characterised by regular minor contents of Ag (2.73–3.72 wt. %) and Cu (0.22–0.34 wt. %). In comparison with published data (e.g. Cook 1997; Putz et al. 2003; Topa and Makovicky 2010), samples from Kutná Hora belong to relatively Ag-rich and Cu-poor cosalite. The regular contents of Sb substituting for Bi (2.67–4.25 wt. %) corresponding to Bi/(Bi + Sb) of 0.84–0.90 were also determined. Similar extents of $SbBi_{-1}$ substitution for cosalite have been reported from numerous localities (e.g. Cook 1997; Putz et al. 2003; Topa and Makovicky 2010). Minor contents of Se (up to 0.16 wt. %) substituting for dominant S were also found.

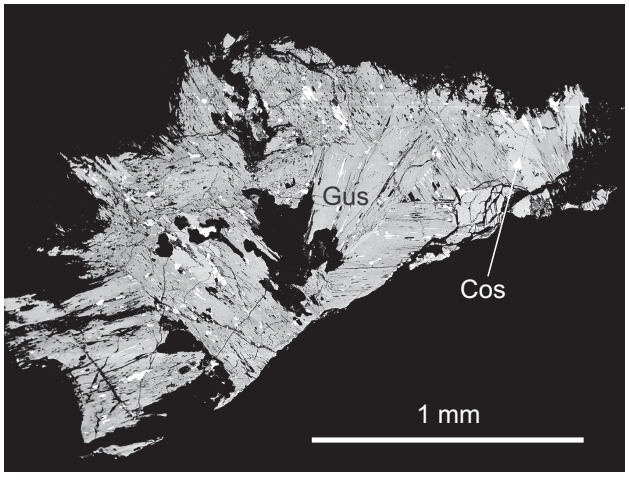

Fig. 6 Back-scattered image of Sb-bearing cosalite (Cos – light grey) associated with undersubstituted gustavite (Gus – medium grey) with a low content of Sb (3.19 wt. %, corresponding to Bi/(Bi + Sb) = 0.89).

Cosalite was not detected in the powder pattern of the samples. No attempt was made to extract the grain for single crystal diffraction from the polished sections due to intimate intergrowth with lillianite homologues and small size of the grains.

4.3. Matildite

Matildite is rare and was found only in three samples as the earliest among the associated Bi minerals. In the first sample (ST 63) it forms grains up to 50 μm intimately intergrown with native Bi, terrywallaceite and aramayoite (Fig. 7a). The second polished section (ST 117) displays two genetically different grains with matildite. In grain one (Fig. 7b) matildite forms anhedral elongated grains up to 100 μm in length and 25 μm in width growing on idiomorphic crystals of galena$_{ss}$. In grain two (Fig. 7c) matildite forms worm-shaped inclusions up to 70 μm across in galena$_{ss}$ replacing native bismuth. The third sample (ST 12 A) is genetically interesting (Fig. 7d) as it features two generations of matildite. Matildite II forms exsolution lamellae up to 40 × 5 μm as decomposition products (together with native bismuth II and galena$_{ss}$ II of unmeasurable size, not marked in image) of eskimoite and Sb-rich gustavite. The crystallization sequence was as follows: native Bi I – galena I – matildite I – eskimoite – matildite II + native Bi II + galena II – Sb-rich gustavite – terrywallaceite.

Chemical composition of matildite from Kutná Hora and corresponding chemical formulae are given in Tab. 4. Most measured points show increased Pb content (1.17–6.80 wt. %) corresponding to 1.03–6.25 mol. % PbS, suggesting a solid solution between matildite and galena (Fig. 7a). Numerous phases with

Tab. 3 Chemical composition of cosalite, aramayoite, bismuthinite and ikunolite from Kutná Hora (wt. % and *apfu*)

	cosalite				aramayoite	bismuthinite					ikunolite	
	ST 13A	ST 71A fr1	ST 62	ST 216 A	ST 63 A	ST 90 B	ST 164 B2	ST 23 Cgr1	ST 23 Cgr2	ST 74 fr2	ST 74	ST 74
n	2	1	3	3	5	4	2	1	2	5	2	3
Bi	38.96	39.67	41.11	38.93	25.82	72.01	76.90	72.43	79.17	78.19	86.30	87.08
Pb	36.98	36.65	36.32	37.27	0.49	0.78	2.28	0.99	0.32	0.30	0.70	0.42
Cu	0.25	0.24	0.22	0.34	0.00	0.15	0.57	0.14	0.01	0.01	0.02	0.03
Fe	0.08	0.12	0.02	0.05	0.02	0.00	0.39	0.00	0.02	0.00	0.02	0.01
Se	0.10	0.03	0.14	0.03	0.09	0.09	0.05	0.16	0.09	0.05	0.08	0.07
S	16.93	17.08	17.06	16.79	18.99	19.99	18.59	19.74	18.77	19.16	9.72	9.88
Sb	3.73	4.25	2.67	3.77	22.60	6.57	0.55	6.37	1.08	1.35	0.00	0.01
Ag	2.73	2.74	3.72	2.77	32.39	0.02	0.01	0.01	0.01	0.01	0.22	0.07
Cd	0.22	0.17	0.16	0.17	0.01	0.00	0.00	0.00	0.00	0.00	0.00	0.16
Te											0.05	0.08
Total	99.98	100.95	101.42	100.13	99.87	99.61	99.35	99.84	99.47	99.07	97.11	97.80
apfu	36				12	5					7	
Bi	7.01	7.06	7.32	7.02	1.23	1.67	1.88	1.69	1.94	1.90	4.00	3.99
Pb	6.71	6.58	6.52	6.78	0.02	0.02	0.06	0.02	0.01	0.01	0.03	0.02
Cu	0.15	0.14	0.13	0.02	0.00	0.01	0.05	0.01	0.00	0.00	0.00	0.01
Fe	0.05	0.08	0.01	0.03	0.00	0.00	0.04	0.00	0.00	0.00	0.00	0.00
Se	0.05	0.01	0.07	0.01	0.01	0.01	0.00	0.01	0.01	0.00	0.01	0.01
S	19.85	19.82	19.8	19.75	5.92	3.03	2.96	3.01	3.00	3.03	2.93	2.95
Sb	1.15	1.03	0.81	1.17	1.81	0.26	0.02	0.26	0.05	0.06	0.00	0.00
Ag	0.95	0.95	1.28	0.97	3.00	0.00	0.00	0.00	0.00	0.00	0.02	0.01
Cd	0.07	0.05	0.05	0.06	0.00	0.00	0.00	0.00	0.00	0.00	0.00	0.01
Te											0.00	0.01
Bi/(Bi + Sb)	0.86	0.84	0.90	0.86	0.41	0.86	0.99	0.87	0.98	0.97		
n_{aik}						1.90	5.80	2.40	0.80	0.80		

apfu – atoms per formula unit – the basis for calculation of the empirical formula
n – number of point analyses
n_{aik} – hypothetical percentage of the aikinite end member

Tab. 4 Chemical composition matildite from Kutná Hora (wt. % and formula coefficients based on 4 *apfu*)

	ST 63 A	ST 117 gr1	ST 117 gr2	ST 12 A	ST 12 A	ST 12 A	ST 12 A
n	2	5	2	5	8	3	2
Bi	51.70	53.81	51.92	53.58	52.28	50.95	49.97
Pb	1.17	1.65	4.32	0.38	2.82	5.09	6.80
Cu	0.00	0.01	0.01	0.00	0.00	0.00	0.00
Fe	0.47	0.00	0.00	0.01	0.01	0.00	0.00
Se	0.05	0.11	0.07	0.00	0.00	0.00	0.00
S	16.68	17.49	17.65	16.37	16.05	16.01	16.07
Sb	4.11	0.15	0.17	0.09	0.18	0.13	0.12
Ag	27.20	26.70	27.41	28.46	27.40	27.37	27.15
Cd	0.52	0.11	0.13	0.00	0.00	0.00	0.00
Total	101.91	100.03	101.69	98.90	98.75	99.56	100.12
Bi	0.92	0.97	0.92	0.99	0.98	0.95	0.93
Pb	0.02	0.03	0.08	0.01	0.05	0.10	0.13
Cu	0.00	0.00	0.00	0.00	0.00	0.00	0.00
Fe	0.03	0.00	0.00	0.00	0.00	0.00	0.00
Se	0.00	0.01	0.00	0.00	0.00	0.00	0.00
S	1.94	2.05	2.04	1.98	1.96	1.95	1.95
Sb	0.13	0.00	0.01	0.00	0.01	0.00	0.00
Ag	0.94	0.93	0.94	1.02	1.00	0.99	0.98
Cd	0.02	0.00	0.00	0.00	0.00	0.00	0.00
Bi/(Bi + Sb)	0.88	1.00	0.99	1.00	0.99	1.00	1.00
mol. % PbS	1.03	1.54	3.96	0.39	2.67	4.70	6.25

n – number of point analyses
for each sample, analyses are ordered according to the increasing Pb contents

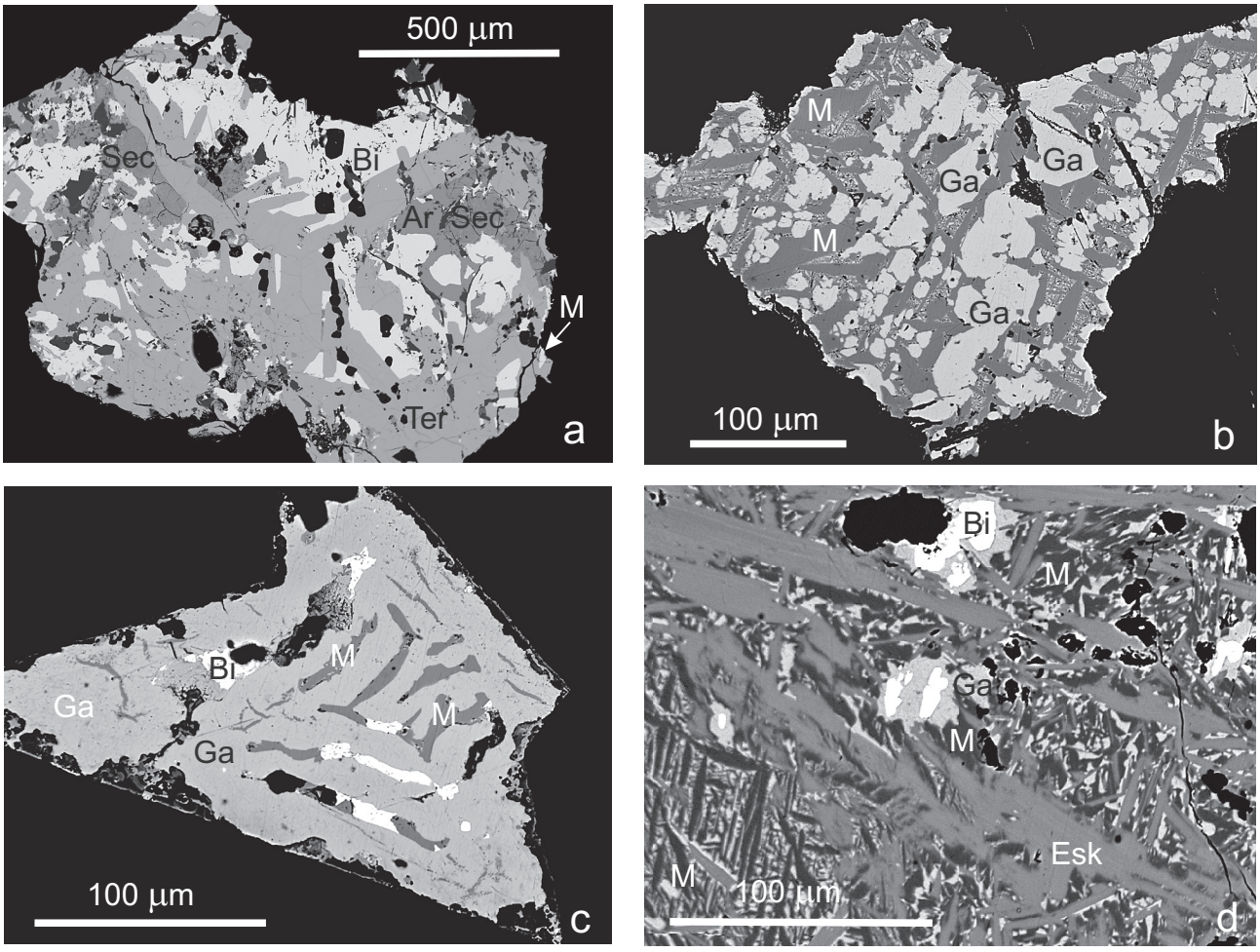

Fig. 7a – Allotriomorphic grains of Sb-bearing matildite (M), homogenous terrywallaceite (Ter), aramayoite (Ar – darker grey), an unidentified supergene phase (Sec – even darker grey) and native Bi (white). BSE image of sample ST 63. **b** – Anhedral elongated grains of matildite (M, dark) growing on idiomorphic crystals of Ag, Bi-galena (Ga). BSE image of sample ST 117 gr 1. **c** – Worm-shaped inclusions of matildite up to 70 µm long in galena$_{ss}$ replacing native bismuth. BSE image of sample ST 117 gr2. **d** – Grains of native Bi I (Bi - white) with galena I (Ga – light grey) and adjacent matildite I (M – dark grey). Matildite II forms exsolution lamellae up to 40 × 5 µm as decomposition products (together with native bismuth II and galena$_{ss}$ II of unmeasurable size, not marked in image) of eskimoite (Esk, medium grey) and Sb-rich gustavite (not in picture). BSE image of sample ST 12 A.

intermediate compositions along the $AgBiS_2$–PbS join have been described on the basis of chemical composition (e.g. Kovalenker et al. 1993; Damian et al. 2008; Voudouris et al. 2013) but none of them has been approved as a new mineral due to the lack of structural data. The only two exceptions are high-temperature schapbachite ($Ag_{0.4}Pb_{0.2}Bi_{0.4}S$) stabilized by Pb content (Walenta et al. 2004; Staude et al. 2010) and problematic schirmerite (Type I) ($Ag_4PbBi_4S_9$) (Moëlo et al. 2008). Increased Sb content [Bi/(Bi + Sb) = 0.88] was observed only in the sample ST 63 where Sb-rich matildite is associated with terrywallaceite and native bismuth but without galena.

The determination of matildite was confirmed by the PXRD, unit-cell parameters refined for the space group *P*-3*m*1 are compared in the Tab. 5 with published data of this mineral phase.

4.4. Galena solid solution (PbS_{ss})

Galena occurs frequently in most samples with Bi- and Bi–Sb sulphosalts. Galena belongs to the oldest Bi-bear-

Tab. 5 Unit cell parameters of matildite for trigonal space group *P*-3*m*1

Sample		*a* [Å]	*c* [Å]	V [Å^3]
Kutná Hora (ST 63A)	this paper	4.178(2)	19.81(1)	299.50
synt.	Geller and Wernick (1959)	4.184(5)	19.78(2)	299.90

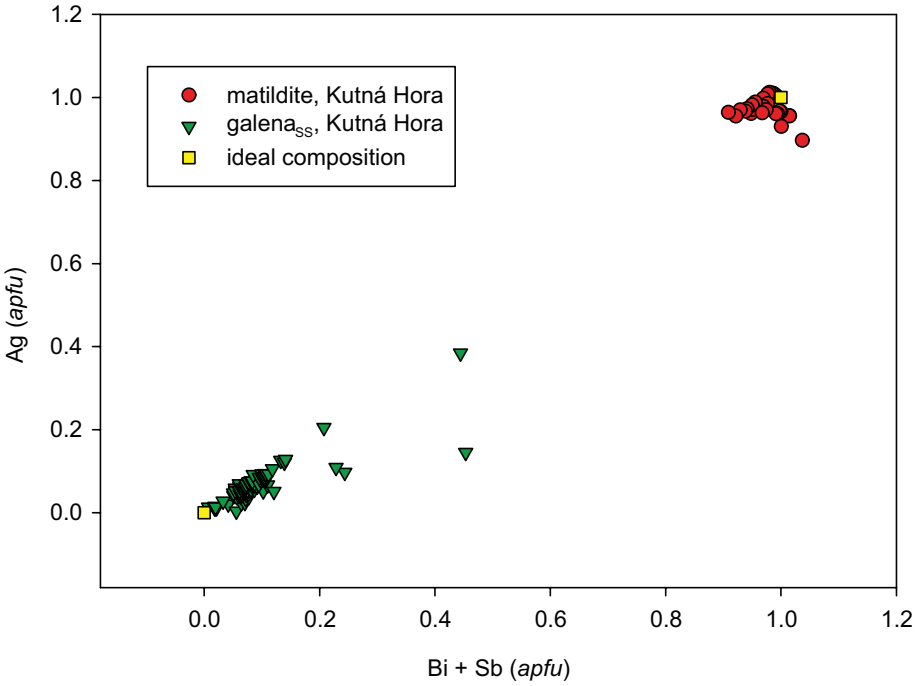

Fig. 8 Graph Bi + Sb vs. Ag (apfu) for minerals along galena–matildite join (calculation based on 4 apfu).

ing minerals, it often forms large corroded xenomorphic grains several hundred microns across with distinct cleavage, which is often followed by replacing minerals. Galena relics occur frequently inside aggregates of younger lamellae of Bi-bearing lillianite homologues (gustavite, vikingite, treasurite, eskimoite).

The chemical composition of galena associated with lillianite homologues or other Bi-bearing sulphosalts is characterized by increased contents of Ag and Bi (Electronic Supplementary Material 1). Neither optical microscopy nor back-scattered electron (BSE) images revealed microscopic inclusions of other phases. A good correlation of Ag and Bi (Fig. 8) suggests that the studied galena samples are members of the galena–matildite (PbS–$AgBiS_2$) solid solution series, referred to as PbS_{ss} (e.g., Foord et al. 1988; Foord and Shawe 1989).

The maximum values of Ag and Bi in the PbS_{ss} grains are 9.44 and 21.02 wt. % respectively, corresponding to 0.20 Ag and 0.23 Bi *apfu*. Such a high degree of substitution was observed only in one grain (Fig. 8) and corresponds to the highest known contents of Ag in PbS_{ss} (Foord et al. 1988; Wang 1999; Staude et al. 2010). In most studied PbS_{ss} grains the contents of Ag do not exceed 0.10 *apfu*; similar range of Ag + (Bi,Sb) → 2Pb substitution in PbS_{ss} are known from other occurrences in the world (e.g. Foord et al. 1988; Foord and Shawe 1989; Staude et al. 2010). In some grains Bi exceeds Ag (Fig. 8), suggesting another substitution, not coupled with Ag, most probably 2(Bi,Sb) + □ → 3Pb (George et al. 2015).

4.5. Aramayoite

Aramayoite was found only in one polished section (sample ST 63A). It forms irregular aggregates up to 200 µm in size replacing earlier native bismuth and idiomorphic grains of terrywallaceite (Fig. 7a). The succession of associated mineral phases was: native bismuth → matildite → terrywallaceite → aramayoite → unspecified supergene phase.

The chemical composition of aramayoite from Kutná Hora and corresponding chemical formula are presented in Tab. 3. The ideal formula of aramayoite is $Ag_3Sb_2(Bi,Sb)S_6$; the Sb/Bi ratio in natural samples varies between 1.44 and 4.27 (Effenberger et al. 2002). The studied sample with the Sb/Bi of 1.44–1.50 [i.e., Bi/(Bi + Sb) = 0.41] thus belongs to the Bi-richest aramayoite, resembling the samples from Altenberg, Austria (Effenberger et al. 2002; Putz et al. 2003). The determination of aramayoite was confirmed by the PXRD, unit-cell parameters refined for the space group *P*-1 are compared in the Tab. 6 with published data for this mineral phase.

4.6. Bismuthinite

Bismuthinite forms irregular grains up to 50 µm usually replacing native bismuth. It also occurs in association with, much more frequent, lillianite homologues. Only in one sample (ST 90 B) it forms large irregular grains up to 200 µm replacing native bismuth, itself being replaced by terrywallaceite.

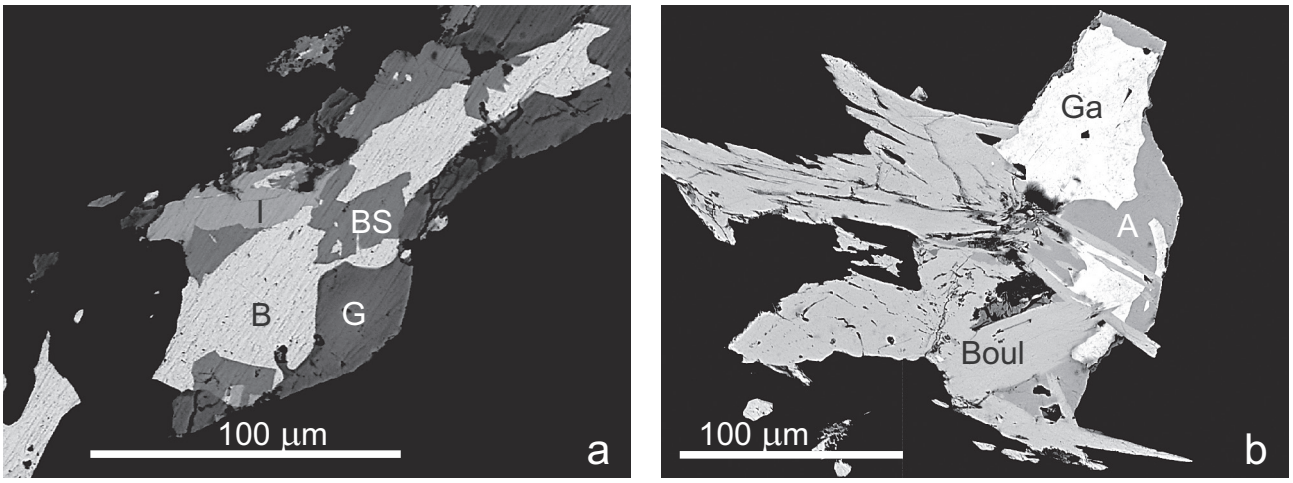

Fig. 9a – Ikunolite (I – light grey) associated with native bismuth (B – white), bismuthinite (BS – medium grey) and Sb-gustavite (G – dark grey). BSE image of the sample ST 74. **b –** Bi-rich boulangerite (Boul) replacing earlier galena$_{ss}$ (Ga). Both phases are being replaced by the latest allotriomorphic grains of Bi-rich phase $^{5}And_{69}$ (A). BSE image of sample ST 104gr1.

Chemical compositions of bismuthinite from Kutná Hora and corresponding chemical formulae are given in Tab. 3. The empirical formula $Cu_xPb_yBi_{8-1/2(x+y)}S_{12}$ was used for calculation of bismuthinite on the basis of (Cu + Pb)/2 + Bi = 8 *apfu*, after Makovicky and Makovicky (1978). The position in the bismuthinite–aikinite series is described by the percentage of the hypothetical aikinite end member n_{aik} = [2 Pb/(Pb + Bi)] × 100. Two substitutions are present in studied samples:
(1) $Bi^{3+} \leftrightarrow Sb^{3+}$; two samples are Sb-rich varieties with Bi/(Bi + Sb) = 0.86–0.87 (with Sb content up to 6.57 wt. %), corresponding to approximately one atom of Sb substituting for Bi per unit cell. Three other samples are almost Sb-free with Bi/(Bi + Sb) = 0.98–0.99.
(2) Weak aikinite substitution: $Cu^{+} + Pb^{2+} \leftrightarrow Bi^{3+} + \square$; calculated values of n_{aik} = 0.8–6.1 are above the solid-solution field of bismuthinite–aikinite series (e.g. Topa et al. 2002; Cook and Ciobanu 2003). Pure bismuthinite has n_{aik} = 0, pekoite ($CuPbBi_{11}S_{18}$), the first mineral of the bismuthinite–aikinite series, has n_{aik} = 17.

4.7. Ikunolite

Ikunolite was found only in one sample as irregular elongated grains up to 70 µm in length (Fig. 9a) replacing native Bi, itself being replaced by bismuthinite. The crystallization sequence was: native Bi → ikunolite → bismuthinite → terrywallaceite/Sb-rich gustavite.

Its chemical composition (Tab. 3, Fig. 10a) corresponds to a phase with formula Bi_4S_3, i.e. Se-free ikunolite. Analyses showed low totals (between 96.79–98.21 wt. %) which could be explained by the presence of other, not measured elements. Therefore, a complete WD scan of all elements from oxygen onwards was carried out with the emphasis on O and Cl. No elements were detected except for oxygen, which is nonetheless questionable due to the omnipresent oxidation films on surfaces of polished sections.

Ikunolite from Kutná Hora is virtually a Se-free member (Fig. 10a) of Bi_4S_3–$Bi_4S_{1.5}Se_{1.5}$ solid solution (Parafiniuk et al. 2008). Similar Se-free ikunolite was described from Kingsgate, Australia (Markham 1962), Yeonhwa Mine, South Korea (Imai and Chung 1986), Stanos, Greece (Voudouris et al. 2013) or the Stan Terg deposit, Kosovo (Kołodziejczyk et al. 2015).

4.8. Bi-bearing Pb–Sb sulphosalts

The Pb–Sb sulphosalts occur frequently among ore minerals in quartz gangue of the Kutná Hora deposit, but they normally contain no bismuth. However, the newly described Bi and Bi–Sb sulphosalt mineralization was found to include the same Pb–Sb sulphosalts but with significantly increased contents of bismuth.

Tab. 6 Unit cell parameters of aramayoite for triclinic space group P-1

		a [Å]	*b* [Å]	*c* [Å]	*a* [°]	*b* [°]	*γ* [°]	V [Å^3]
Staročeské pásmo Lode, Kutná Hora	this paper	7.800(13)	8.255(11)	8.874(11)	100.13(10)	103.99(10)	90.26(10)	545.10
Armonia mine, El Quevar, Argentina	Effenberger et al. (2002)	7.813(2)	8.268(2)	8.880(2)	100.32(2)	104.07(2)	90.18(2)	546.76
Animas mine, Potosi, Bolivia	Mullen and Nowacki (1974)	7.76(2)	8.23(2)	8.85(2)	100.2(2)	103.8(2)	90.7(2)	539.5

Tab. 7 Chemical composition of B-rich jamesonite from Kutná Hora (wt. % and formula coefficients based on 25 *apfu*)

	ST 61 B	ST 59 D	ST 42 E	ST 23 B fr1	ST 49 D gr1	ST 30 A gr2	ST 120 A fr2	ST 27 A	ST 54 A	ST 42 C gr1	ST 23 B fr1	ST 67 B gr1	ST 89 B	ST 120 A fr2	ST 30 A gr2
n	1	1	2	1	4	2	3	2	1	1	1	1	1	7	2
Bi	1.35	1.62	3.88	3.88	3.94	4.69	5.54	6.00	7.01	6.80	8.35	8.72	8.85	8.95	10.10
Pb	39.74	40.04	40.01	38.79	38.94	39.20	38.61	39.44	39.03	39.69	38.49	38.41	39.74	38.49	38.56
Cu	0.00	0.00	0.00	0.00	0.05	0.00	0.01	0.01	0.00	0.00	0.00	0.00	0.00	0.01	0.01
Fe	2.60	2.54	2.56	2.55	2.65	2.54	2.47	2.55	2.49	2.61	2.40	2.53	2.50	2.43	2.46
Se	0.00	0.09	0.05	0.07	0.06	0.08	0.00	0.07	0.03	0.05	0.05	0.06	0.06	0.01	0.05
S	21.54	22.03	21.12	21.93	20.97	21.13	21.98	22.10	20.75	20.67	21.07	21.07	19.90	21.28	20.76
Sb	33.87	34.04	33.41	33.16	31.55	31.81	32.13	31.72	30.72	29.63	29.75	28.86	28.78	29.75	27.75
Ag	0.00	0.00	0.00	0.00	0.00	0.00	0.01	0.00	0.00	0.00	0.01	0.00	0.00	0.02	0.17
Cd	0.00	0.00	0.00	0.00	0.00	0.00	0.00	0.00	0.00	0.00	0.00	0.00	0.00	0.00	0.00
Total	99.09	100.37	101.03	100.39	98.17	99.44	100.83	101.88	100.03	99.44	100.12	99.64	99.83	101.00	99.76
Bi	0.13	0.16	0.39	0.38	0.40	0.48	0.55	0.59	0.72	0.70	0.85	0.89	0.93	0.91	1.04
Pb	4.01	3.98	4.05	3.87	4.02	4.10	3.86	3.92	4.04	4.13	3.97	3.97	4.22	3.93	4.03
Cu	0.00	0.00	0.00	0.00	0.02	0.00	0.00	0.00	0.00	0.00	0.00	0.00	0.00	0.00	0.00
Fe	0.97	0.94	0.96	0.94	1.01	0.96	0.91	0.94	0.95	1.01	0.92	0.97	0.98	0.92	0.95
Se	0.00	0.02	0.01	0.02	0.02	0.02	0.00	0.02	0.01	0.01	0.01	0.02	0.02	0.00	0.01
S	14.60	14.14	13.82	14.15	13.99	13.98	14.19	14.18	13.87	13.90	14.03	14.07	13.65	14.04	14.01
Sb	5.82	5.76	5.76	5.63	5.54	5.54	5.46	5.36	5.41	5.25	5.22	5.08	5.20	5.17	4.93
Ag	0.00	0.00	0.00	0.00	0.00	0.00	0.00	0.00	0.00	0.00	0.00	0.00	0.00	0.00	0.03
Cd	0.00	0.00	0.00	0.00	0.00	0.00	0.00	0.00	0.00	0.00	0.00	0.00	0.00	0.00	0.00
Bi/(Bi + Sb)	0.02	0.03	0.06	0.06	0.07	0.08	0.09	0.10	0.12	0.12	0.14	0.15	0.15	0.15	0.17

Tab. 7 Continued

	ST 120 A fr2	ST 42 E	ST 27 B	ST 81 B2	ST 27 A	ST 81 B	ST 120 A fr2	ST 54 A	ST 27 B	ST 120 A fr2	ST 55 gr1	ST 120 A fr2	ST 120 A fr2
n	3	2	2	1	3	2	2	1	1	2	1	1	1
Bi	10.40	10.35	10.21	10.39	11.52	11.85	12.82	13.27	13.68	14.73	15.04	16.50	17.98
Pb	38.38	39.00	38.95	38.65	38.89	37.95	38.29	37.69	38.58	37.66	37.53	37.76	37.40
Cu	0.01	0.00	0.00	0.00	0.02	0.01	0.01	0.00	0.00	0.01	0.00	0.00	0.00
Fe	2.42	2.42	2.45	2.41	2.46	2.50	2.38	2.40	2.42	2.37	2.44	2.32	2.30
Se	0.00	0.08	0.09	0.08	0.08	0.01	0.00	0.06	0.02	0.00	0.04	0.00	0.00
S	20.99	20.37	21.62	20.28	21.00	20.16	21.22	20.63	21.34	20.43	21.29	21.16	21.08
Sb	28.69	28.05	27.56	27.68	26.53	26.44	27.15	26.86	25.14	25.42	24.98	24.49	23.42
Ag	0.01	0.00	0.00	0.00	0.01	0.02	0.00	0.00	0.00	0.00	0.00	0.00	0.00
Cd	0.00	0.00	0.00	0.00	0.00	0.02	0.00	0.00	0.00	0.00	0.00	0.00	0.00
Total	100.97	100.28	100.88	99.49	100.51	98.95	101.94	100.91	101.19	100.68	101.32	102.31	102.23
Bi	1.06	1.08	1.04	1.09	1.19	1.25	1.31	1.38	1.40	1.54	1.54	1.69	1.86
Pb	3.96	4.10	3.97	4.10	4.04	4.05	3.93	3.94	3.99	3.98	3.88	3.91	3.90
Cu	0.00	0.00	0.00	0.00	0.01	0.00	0.00	0.00	0.00	0.00	0.00	0.00	0.00
Fe	0.93	0.95	0.93	0.95	0.95	0.99	0.91	0.93	0.93	0.93	0.94	0.89	0.89
Se	0.00	0.02	0.02	0.02	0.02	0.00	0.00	0.02	0.01	0.00	0.01	0.00	0.00
S	13.99	13.84	14.26	13.89	14.10	13.90	14.09	13.95	14.25	13.95	14.23	14.16	14.19
Sb	5.04	5.02	4.78	4.99	4.69	4.80	4.75	4.78	4.42	4.57	4.40	4.32	4.15
Ag	0.00	0.00	0.00	0.00	0.00	0.00	0.00	0.00	0.00	0.00	0.00	0.00	0.00
Cd	0.00	0.00	0.00	0.00	0.00	0.00	0.00	0.00	0.00	0.00	0.00	0.00	0.00
Bi/(Bi + Sb)	0.17	0.18	0.18	0.18	0.20	0.21	0.22	0.22	0.24	0.25	0.26	0.28	0.31

n – number of point analyses
analyses are ordered according to the Bi/(Bi + Sb) ratios

4.8.1. Bi-rich jamesonite

Significant amounts of Bi were found in jamesonite, which often forms characteristic needle-like aggregates up to 200 × 300 µm concentrated along the rims of older grains of lillianite homologues and izoklakeite (Fig. 3).

The chemical composition of the studied jamesonite (Tab. 7, Fig. 10b) is characterized by increased contents of Bi (0.13–1.86 *apfu*). Similar Bi contents were published from other occurrences of jamesonite, e.g. from Brezno-Hviezda (Pršek et al. 2008) or Kasejovice (Litochleb 1998). Bismuth contents in jamesonite may reach up to 3 *apfu* (a questionable mineral species named *sakharovaite*). A strong partitioning in the substitution of Bi among the three Sb positions in the jamesonite crystal structure cannot be excluded (similar to garavellite) but its confirmation by single crystal diffraction is missing (Moëlo et al. 2008).

Therefore, the structure of bismuthian jamesonite with 15 wt % of Bi from the Staročeské pásmo Lode was attempted with the aim to find out whether the Bi distribution at particular Sb sites in the structure of the mineral warrants a new mineral species. The attempts showed that Bi atoms are placed randomly with no preference for any of Sb sites. Even though the Bi content was theoretically high enough to predominate over Sb if concentrated in a single site, this is not the case for the measured Bi-rich jamesonite. This phase is therefore not entitled to become a new mineral species.

4.8.2. Bi-rich boulangerite

Bi-rich boulangerite was found as acicular to prismatic crystals up to 200 µm in length (Fig. 9b) in association with the Bi-rich andorite phase and galena$_{ss}$. The earliest mineral was galena$_{ss}$, later replaced by Bi-rich boulangerite. The youngest was the andorite phase with N = 5 (^{5}And$_{69}$), a possible Sb-analogue of vikingite (Pažout 2017). In the other two samples, the earliest mineral was

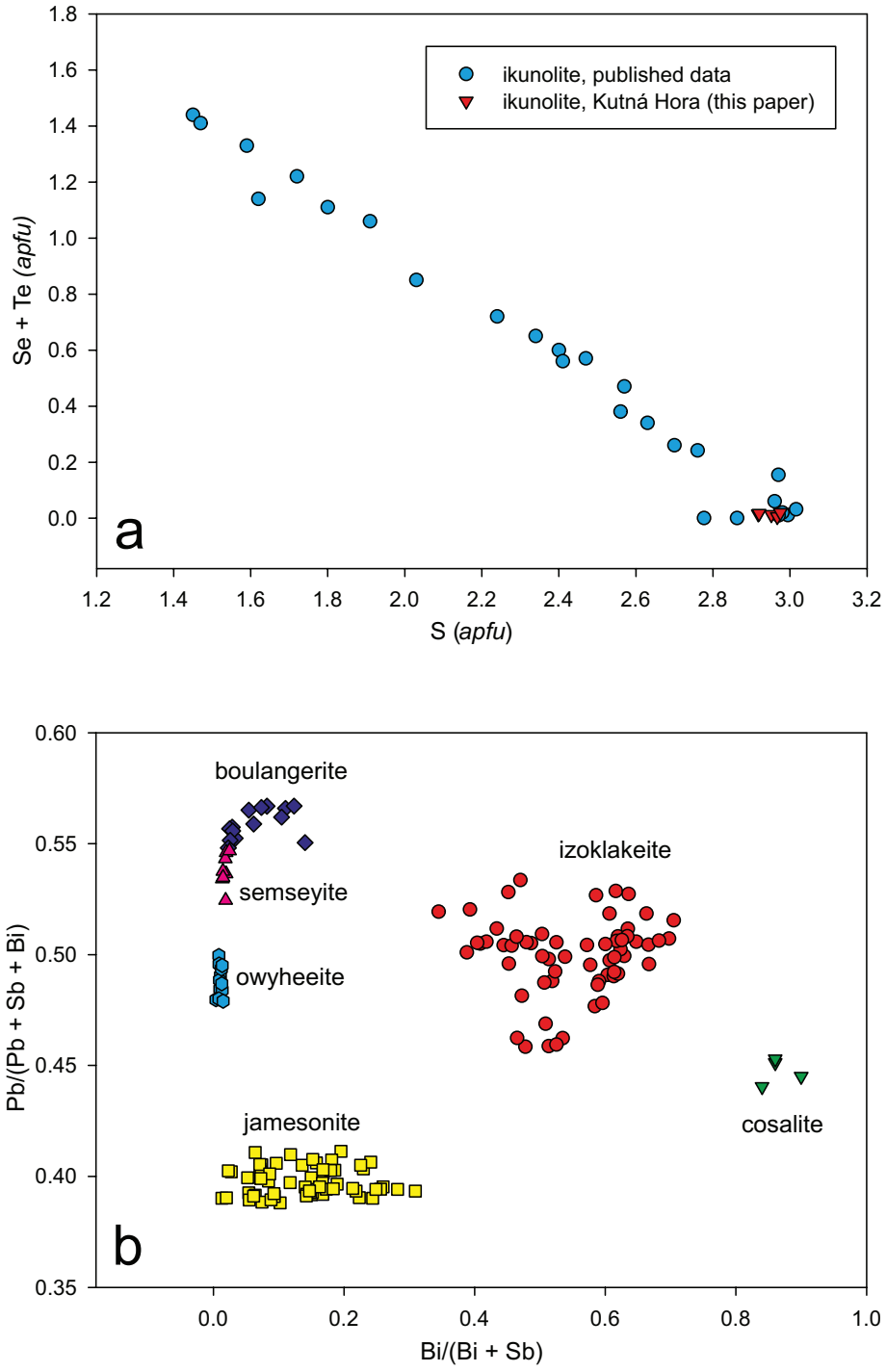

Fig. 10a – Graph S vs. Se + Te (*apfu*) for ikunolite; published data for ikunolite are from Kato (1959), Markham (1962), Imai and Chung (1986), Parafiniuk et al. (2008) and Voudouris et al. (2013). **b** – Bi/(Bi + Sb) vs. Pb/(Pb + Sb + Bi) graph for the studied Pb-(Sb,Bi) sulfosalts from Kutná Hora.

Tab. 8 Chemical composition of Bi-rich boulangerite, Bi-bearing semseyite and Bi-bearing owyheeite from Kutná Hora (wt. % and *apfu*)

	boulangerite					semseyite	owyheeite		
	ST 109	ST 109	ST 104	ST 104	ST 89 B	ST 170 E	ST 136 A2	ST 136 A2	ST 136 A2
Instrument	s	p	s	p		c			
n	2	4	2	2	1	8	3	5	3
Bi	1.18	1.24	4.05	4.85	6.18	0.83	0.44	0.51	0.43
Pb	54.72	54.41	54.51	54.45	53.43	53.97	45.58	44.52	44.81
Cu	0.03	0.14	0.02	0.02	0.00	0.01	0.04	0.08	0.01
Fe	0.07	0.01	0.01	0.04	0.02	0.05	0.07	0.03	0.11
Se	0.08	0.02	0.05	0.03	0.00	0.15	0.22	0.25	0.22
S	18.70	18.81	18.27	18.35	17.97	19.25	18.85	18.48	19.03
Sb	25.00	25.27	22.19	21.98	22.09	26.85	26.88	27.13	28.32
Ag	0.03	0.04	0.00	0.06	0.00	0.00	6.54	6.92	6.88
Cd	0.00	0.02	0.00	0.07	0.00	0.00	0.00	0.05	0.01
Total	99.80	99.96	99.09	99.85	99.69	101.11	98.63	97.96	99.81
apfu			20			38		52	
Bi	0.11	0.11	0.37	0.45	0.57	0.14	0.10	0.12	0.10
Pb	4.98	4.93	5.08	5.05	5.01	9.10	10.44	10.30	10.10
Cu	0.01	0.04	0.01	0.01	0.00	0.00	0.04	0.06	0.02
Fe	0.02	0.00	0.00	0.01	0.01	0.03	0.06	0.02	0.10
Se	0.02	0.00	0.01	0.01	0.00	0.07	0.14	0.14	0.12
S	10.99	11.02	11.00	11.00	10.89	20.96	27.88	27.60	27.74
Sb	3.87	3.90	3.52	3.47	3.52	7.70	10.48	10.68	10.86
Ag	0.01	0.01	0.00	0.01	0.00	0.00	2.88	3.08	2.98
Cd	0.00	0.00	0.00	0.01	0.00	0.00	0.00	0.02	0.00
Bi/(Bi + Sb)	0.03	0.03	0.11	0.11	0.14	0.02	0.01	0.01	0.01

apfu – atoms per formula unit – the basis for calculation of the empirical formula
n – number of point analyses
analyses are ordered according to the Bi/(Bi + Sb) ratios
s – Jeol electron microprobe in Salzburg
p – Cameca electron microprobe in Prague
c – analysis of Pažout (2008)

galena$_{ss}$, replaced by Bi-rich boulangerite, and overgrown by the latest Bi-rich jamesonite.

The chemical composition and chemical formula of boulangerite from Kutná Hora are given in Tab. 8. The extent of Bi for Sb substitution (0.11–0.57 *apfu*) is far more limited than for jamesonite (Fig. 10b). Comparable contents of Bi in boulangerite are rare worldwide, but they are known e.g. from the Srednegolgota deposit, Transbaikalia (Bortnikov and Tsepin 1987), Apollo mine, Germany (Wagner and Cook 1996) or the Damajianshan deposit, China (Zhang et al. 2015).

4.8.3. Bi-bearing semseyite

Bi-bearing semseyite was found in one sample as grey black metallic aggregates up to 4 mm across in association with boulangerite, jamesonite, freibergite and chalcopyrite determined by PXRD (Pažout 2008). It forms needle-like hypidiomorphic aggregates up to 200 μm in size intergrown with older irregular grains of galena$_{ss}$. Contents of Bi (Fig. 10b) range between 0.65 and 1.12 wt. % (0.11–0.19 *apfu*). In BSE images, the changes in Bi content show as darker lath-shaped zones of Bi-poorer semseyite within lighter lamellae of Bi-richer semseyite. Increased contents of Se up to 0.22 wt.% were also determined (Tab. 8). Occurrences of Bi-bearing semseyite are known only from Apollo mine, Germany (Wagner and Cook 1996, 1997), where up to 8.5 wt. % Bi was detected.

4.8.4. Bi-bearing owyheeite

Bi-bearing owyheeite was found only in one sample although "normal" (Bi-free) owyheeite is a fairly frequent mineral throughout the ore district. Needles of Bi-bearing owyheeite form irregular clusters up to 150 μm across in quartz, associated with diaphorite (up to 0.12 wt. % of Bi), galena (up to 0.22 wt. % of Bi and 0.30 wt. % of Ag), both enclosed in arsenopyrite. The chemical composition of owyheeite from Kutná Hora and corresponding chemical formula are given in Tab. 8. Lower totals in two groups of analyses are caused by uneven surface at the rim of the grain in quartz matrix. In comparison with the ideal formula of owyheeite $Ag_3Pb_{10}Sb_{11}S_{28}$ (Moëlo et al. 1984), the studied sample shows a surplus of lead and a deficit of antimony. A similar situation was described by

Laufek et al. (2007) for owyheeite from the neighbouring Turkaňkské pásmo Lode (also in the northern part of the Kutná hora ore district). The contents of bismuth in the studied owyheeite are relatively low (Fig. 10b) (0.19–0.71 wt. %; 0.04–0.16 *apfu*).

5. Discussion

Kutná Hora ore district is considered a typical example of postmagmatic sulphide base-metal mineralization of late Variscan age (Early Permian; Bernard 1991), analogous to the "*kb + eb"* mineralizations of Freiberg in Saxony (Bernard 1961). The ore mineralization of the Kutná Hora district originated at several stages, separated by tectonic movements. The first two stages (arsenopyrite/stannite/pyrrhotite and galena/tetrahedrite/jamesonite) are characteristic of the northern "pyrite-rich" lodes. The third stage (miargyrite/freibergite/berthierite) typifies the southern "silver-rich" lodes (Bernard and Pouba 1986).

Silver minerals in both parts of the ore district occur mostly on independent younger structures within the vein system; marked differences between the southern and northern lodes are primarily caused by a different geological (petrological, tectonic) structure of both parts (Holub et al. 1982). Bernard and Žák (1992) suggested that mineralization of Kutná Hora ore district had temporal and genetic relationships to the Variscan metamorphism and magmatism and originated generally at high temperatures (430 ± 80 °C); younger parts of the mineralization were colder (< 190 °C, Žák et al. 1993).

Similar formation temperatures (early high-T of *c.* 400–500 °C; later intermediate-T of *c.* 200–350 °C) were given for analogous mineralizations of the Českomoravská vrchovina Upland (Malý and Dolníček 2005). For Freiberg deposit, Seifert and Sandmann (2006) estimated formation temperatures of the *kb* mineralization at 370 °C (250–410) and of the *eb* mineralization at 250 °C (120–300).

Moreover, the frequent occurrence of native Bi (melting point 271 °C; Živkovič and Živkovič 1996) and the presence of exsolution textures of matildite and galena$_{ss}$ (< 144 °C; Wang 1999; Staude et al. 2010) further constrain the origin of the newly found mineral association of Pb–Bi–Sb–Ag sulphosalts from the Staročeské pásmo Lode to *c.* 100–250 °C. It was thus considerably colder than the earlier high-T base sulphides mineralization of the Staročeské pásmo Lode and corresponds to the lower limit of the younger mineralizations typical of the southerly (Ag-rich) lodes of the Kutná Hora ore district (Oselské pásmo and Roveňské pásmo lodes).

The following groups of Bi-bearing minerals typify the mineralogical composition of the studied mineral paragenesis of the Ag–Pb–Bi–Sb sulphosalts of the Kutná Hora ore district: members of the lillianite homologous series with an extraordinarily variable extent of the Sb for Bi substitution (Pažout 2017), Sb-rich Pb–Bi sulphosalts, Bi-rich Pb–Sb sulphosalts and other Bi-bearing phases (aramayoite, matildite, bismuth and galena$_{ss}$). Thus, this mineral association differs considerably not only from the earlier high-T base-metal mineralization of the northern (pyrite-rich) lodes, but also from relatively low-T mineralization of the southern Ag-rich lodes (where no Bi was detected).

It can be assumed that the origin of this sulphosalt mineralization was related to the penetration of relatively low-T (*c.* 100–250 °C) hydrothermal fluids into newly tectonically opened fractures in earlier (older) filling of ore veins of the Staročeské pásmo Lode (Bernard and Žák 1992; Mikuš et al. 1994; Šrein and Pažout 2002). With regard to the movements of fluids in newly opened fractures and their lower temperature, virtually no mobilization of elements from the earlier vein filling took place. Almost complete absence of Cu (except for izoklakeite) and a lack of As and Sn, which are all frequently present in the earlier (older) vein mineralization, are characteristic of the studied bismuth sulphosalt association.

The inferred chemical composition of the fluids significantly differs from the mineralization known from the southern (Ag-rich) lodes of the Kutná Hora ore district. The studied mineralization apparently originated in an environment rich in Ag and Pb and, therefore, miargyrite is rare although it is very frequent in the southern lodes. Simultaneously it was very poor in Cu, and thus freibergite, although it is common throughout the ore district and was also present in the early sulphide stage, is missing. An environment very poor in Cu is testified by low Cu contents in izoklakeite and by the absence of minerals of pavonite and cuprobismutite homologous series, and of sulphosalts such as kobellite, berryite, neyite or angelaite. An origin of certain groups of sulphosalts (e.g. members of pavonite and cuprobismutite homologous series) was very probably hindered by the presence of antimony in the hydrothermal fluids.

6. Conclusions

Following a detailed mineralogical research, hitherto unknown association of Pb–Bi–Sb–Ag sulphosalts was identified in samples of the Staročeské pásmo Lode of the Kutná Hora ore district.

Apart from numerous members of lillianite homologous series, new occurrences of aramayoite, bismuthinite, cosalite, ikunolite, izoklakeite, matildite, galena$_{ss}$, Bi-rich

jamesonite, Bi-rich boulangerite, Bi-rich owyheeite and Bi-rich semseyite have been identified. For izoklakeite and aramayoite, these are the first records from the Czech Republic; bismuthinite, cosalite, ikunolite and matildite are newly confirmed mineral species for the Kutná Hora ore district.

An extraordinary extent of the Bi–Sb substitution is characteristic of the studied association. Bi-rich mineralization of this scope has not been previously known from the Kutná Hora ore district.

The studied association significantly differs by its mineral and chemical composition from both the sulphide-rich mineralization of the northern lodes, and the Ag-rich mineralization of the southern lodes of the Kutná Hora ore district. Its origin is related to the penetration of lower temperature fluids (*c.* 10–250 °C) into tectonically opened fractures in older filling of the Staročeské pásmo Lode ore veins. Virtually no mobilization of elements from the earlier vein filling took place; the latter association of sulphosalts shows almost complete absence of Cu (and total lack of As and Sn). Hydrothermal fluids must have been relatively rich in Ag and Pb (as well as in Sb) and poor in Cu. High Bi content was characteristic of the initial stage of the mineralization. Gradually, the Bi/Sb ratio decreased with more Sb-rich minerals precipitating. At the final stage, Bi-rich Pb–Sb sulphosalts with distinctly lower Ag contents crystallized. With regard to occasionally frequent finds of this mineralization in the mine dump material of the Staročeské pásmo Lode, it cannot be ruled out that this type of mineralization with low but regular Ag contents could have been one of the important sources of silver in the Kutná Hora ore district right from the beginnings of mining in the second half of the 13th till the end of the large-scale mining in the beginning of the 17th century.

Acknowledgements. The authors thank Dan Topa (University of Salzburg) for the WDS microprobe measurements, to Jaroslav Maixner (Institute of Chemical Technology, Prague) for help with powder data collection, Zuzana Cílová for EDS analyses. This work was financed by the Czech Science Foundation (GAČR project 15-18917S) to RP and also by the Ministry of Culture of the Czech Republic (DKRVO 2016/01; National Museum 00023272) to JS and Czech Geological Survey (project 223500) to VŠ. The referee, P. Voudouris, as well as handling editor F. Laufek and editor-in-chief V. Janoušek, are acknowledged for comments and suggestions that greatly helped to improve the manuscript.

Electronic supplementary material. The compositions of Ag–Bi-bearing galena from Kutná Hora are available online at the Journal web site (*http://dx.doi.org/10.3190/jgeosci.230*).

References

Armbruster T, Hummel W (1987) (Sb,Bi,Pb) ordering in sulfosalts: crystal-structure refinement of a Bi-rich izoklakeite. Amer Miner 72: 821–831

Bernard JH (1961) Beitrag zum Vergleich der Entwicklung von Mineralassoziationen auf den Erzgängen von Kutná Hora und Freiberg (Sachsen). Věst Ústř Úst geol 36: 289–291

Bernard JH (1991) Empirical Types of Ore Mineralizations in the Bohemian Massif. Geological Survey, Prague, pp 1–181

Bernard JH, Pouba Z (eds) (1986) Ore Deposits and Metallogenesis of the Czechoslovak Part of the Bohemian Massif. Academia, Prague, pp 1–320 (in Czech)

Bernard JH, Žák K (1992) Stable isotope study of Variscan vein Pb–Zn–Ag mineralization of the Bohemian Massif. Explor Mining Geol 1: 81–84

Bindi L, Menchetti S (2005) Garavellite, $FeSbBiS_4$, from the Caspari mine, North Rhine-Westphalia, Germany: composition, physical properties and determination of the crystal structure. Mineral Petrol 85: 131–139

Bortnikov N, Tsepin A (1987) (Sb,Bi)-sulfosalts from Srednegolgota deposit (East Transbaikalia). Iz Akad Nauk SSSR Ser Geol 1: 86–95 (in Russian)

Cook NJ (1997) Bismuth and bismuth–antimony sulphosalts from Neogene vein mineralization, Baia Borsa area, Maramures, Romania. Mineral Mag 61: 387–409

Cook NJ, Ciobanu CL (2003) Lamellar minerals of the cuprobismutite series and related paděraite: a new occurrence and implications. Canad Mineral 41: 441–456

Damian G, Ciobanu CL, Cook NJ, Damian F (2008) Bismuth sulphosalts from the galena–matildite series in the Cremenea vein, Şuior, Baia Mare district, Romania. Neu Jb Mineral, Abh 185: 199–213

Degen T, Sadki M, Bron E, König U, Nénert G (2014) The HighScore suite. Powder Diffr 29: S13–S18

Effenberger H, Paar WH, Topa D, Criddle AJ, Fleck M (2002) The new mineral baumstarkite and a structural reinvestigation of aramayoite and miargyrite. Amer Miner 87: 753–764

Fergusson I F, Rogerson AH, Wolstenholme JFR, Hughes TE, Huyto n A (1987) Firestar-2. A computer program for the evaluation of X-ray powder measurements and the derivation of crystal lattice parameters

Foord EE, Shawe DR (1989) Pb–Bi–Ag–Cu–(Hg) chemistry of galena and some associated sulfosalts. A review and some new data from Colorado, California and Pennsylvania. Canad Mineral 27: 363–382

Foord EE, Shawe DR, Conklin NM (1988) Coexisting galena, PbS_{ss} and sulfosalts: evidence for multiple episodes of mineralization in the Round Mountain and Manharan gold districts, Nevada. Canad Mineral 26: 355–376

Geller S, Wernick JH (1959) Ternary semiconducting compounds with sodium chloride-like structure: $AgSbSe_2$, $AgSbTe_2$, $AgBiS_2$, $AgBiSe_2$. Acta Cryst 12: 46–54

George L, Cook NJ, Ciobanu CL, Eade BP (2015) Trace and minor elements in galena: a reconnaissance LA-ICP-MS study. Amer Miner 100: 548–569

Ghosal S, Sack AR (1999) Bi–Sb energetics in sulfosalts and sulfides. Mineral Mag 63: 723–733

Graeser S, Harris DC (1986) Giessenite from Giessen near Binn, Switzerland: new data. Canad Mineral 24: 19–20

Harris DC, Roberts AC, Criddle AJ (1986) Izoklakeite, a new mineral species from Izok Lake, Northwest Territories. Canad Mineral 24: 1–5

Hoffman V, Trdlička Z (1979) A matildite-similar phase from Kutná Hora, Czechoslovakia. Čas Mineral Geol 24: 42– 43

Hoffman V, Trdlička Z, Šrein V (1989) Sb-gustavite and bournonite from Kutná Hora. Věst Ústř Úst geol 64: 313–316 (in Czech)

Holub M, Hoffman V, Mikuš V, Trdlička Z (1982) Polymetallic mineralization of the Kutná Hora ore district. Sbor Geol Věd, Ložisk Geol Mineral 23: 69–123 (in Czech with English abstract)

Imai N, Chung J (1986) The first Korean occurrence of ikunolite. Mineral J 13: 65–74

Karup-Møller S (1973) A giessenite–cosalite–galena bearing mineral suite from the Bjørkåsen sulphide deposit at Ofoten in northern Norway. Norsk Geologisk Tidsskrift 53: 41–64

Kato A (1959) Ikunolite, a new bismuth mineral from the Ikuno mine, Japan. Mineral J 2: 397–407

Kitakaze A, Itoh H, Komatsu R, Higuchi Y (2012) Baumstarkite from the Koryu Mine, Hokkaido, Japan. Canad Mineral 50: 101–109

Kołodziejczyk J, Pršek J, Melfos V, Voudouris P, Maliqi F, Kozub-Budzyń G (2015) Bismuth minerals from the Stan Terg deposit (Trepça, Kosovo) – mineralogical contribution to the evolution of the deposit. Neu Jb Mineral, Abh 192: 317–333

Kovalenker V, Jelen S, Sandomyrskaya S (1993) Minerals of the system Ag–Cu–Pb–Bi–S from the polymetallic veins of the Štiavnica–Hodruša ore field (Slovakia). Geol Carpath 44: 409–419

Laufek F, Pažout R, Makovicky E (2007) Crystal structure of owyheeite, $Ag_{1.5}Pb_{4.43}Sb_{6.07}S_{14}$: refinement from powder synchrotron X-ray diffraction. Eur J Mineral 19: 557–566

Litochleb J (1998) Mineralogy of Au-bearing mineralization from the Jakub mine near Kasejovice (SW Bohemia). Bull mineral-petrolog Odd Nár Muz (Praha) 6: 100–112

Makovicky E, Karup-Møller S (1986) New data on giessenite from the Bjørkåsen sulfide deposit at Otoften, northern Norway. Canad Mineral 24: 21–25

Makovicky E, Makovicky M (1978) Representation of composition in the bismuthinite–aikinite series. Canad Mineral 16: 405–409

Malec J, Pauliš P (1997) Kutná Hora ore mining district and appearances of past mining and metallurgic activities on its territory. Bull mineral-petrolog Odd Nar Muz (Praha) 4–5: 86–105 (in Czech)

Malý K, Dolníček Z (2005) Pb–Zn–Ag vein mineralization of the central part of the Českomoravská vrchovina Upland (Czech Republic): S, C and O stable isotope study. Bull Geosci 80: 307–319

Markham NL (1962) Plumbian ikunolite from Kingsgate, New South Wales, Amer Miner 47: 1431–1434

Mikuš M, Hušpauer M, Holub M, Holub Z, Holubová V, Rosengranz O (1994) The closing study of the research project "Kutná Hora ore district – the final evaluation of the geological survey of ores. Raw material: Zn, Ag, Cu and Pb ores". Unpublished manuscript, Geofond, Prague, pp 1–300 (in Czech)

Moëlo Y, Mozgova N, Picot P, Bortnikov N, Vrublevskaya Z (1984) Cristallochimie de l'owyheeite: nouvelles données. Tschermaks Mineral Petrogr Mitt 32: 271–284

Moëlo Y, Roger G, Maurel-Palacin D, Marcoux E, Laroussi A (1995) Chemistry of some Pb–(Cu,Fe)–(Sb,Bi) sulfosalts from France and Portugal. Implications for the crystal chemistry of lead sulfosalts in the Cu-poor part of the Pb_2S_2–Cu_2S–Sb_2S_3–Bi_2S_3 system. Mineral Petrol 53: 229–250

Moëlo Y, Makovicky E, Mozgova NN, Jambor JL, Cook N, Pring A, Paar W, Nickel EH, Graeser S, Karup-Møller S, Balic-Zunic T, Mumme WG, Vurro F, Topa D, Bindi L, Bente K, Shimizu M (2008) Sulfosalt systematics: a review. Report of the sulfosalt subcommittee of the IMA Commission on Ore Mineralogy. Eur J Mineral 20: 7–46

Mullen DJE, Nowacki W (1974) The crystal structure of aramayoite $Ag(Sb,Bi)S_2$. Z Kristallogr 139: 54–69

Novák F (1964) The occurrence of native bismuth in the veins of Kutná Hora deposit. Práce Muz Kutná Hora, Geol Výzk Kutnohorska 5: 29–34 (in Czech)

Orlandi P, Moëlo Y, Biagioni C (2010) Lead–antimony sulfosalts from Tuscany (Italy). X. Dadsonite from the Buca della Vena mine and Bi-rich izoklakeite from the Seravezza marble quarries. Period Mineral 79: 113–121

Ozawa T, Saitow A, Hori H (1998) Chemistry and crystallography of Bi-rich izoklakeite from the Otome mine, Yamanashi Prefecture, Japan and discussion of the izoklakeite–giessenite series. Mineral J 20: 179–187

Parafiniuk J, Pieczka A, Gołębiowska B (2008) Compositional data for ikunolite from Rędziny, Rudawy Janowickie, Lower Silesia, Poland. Canad Mineral 46: 1305–1315

Pauliš P (1998) Minerals of Kutná Hora Ore District. Kuttna, Kutná Hora, pp 1–48 (in Czech)

Pažout R (2008) Natural $Pb_9Sb_8S_{21}$ from Kutná Hora, Czech Republic, first occurrence, chemistry and X-ray powder diffraction data. Ceramics – Silikáty 52: 49–53

Pažout R (2017) Lillianite homologues from Kutná Hora ore district, Czech Republic: a case of large-scale Sb for Bi substitution. J Geosci 62: 37–57

Pouchou JL, Pichoir F (1985) "PAP" (φρZ) procedure for improved quantitative microanalysis. In: Armstrong JT (ed) Microbeam Analysis. San Francisco Press, pp 104–106

Pršek J, Ozdín D, Sejkora J (2008) Eclarite and associated Bi sulfosalts from Brezno-Hviezda occurrence (Nízké Tatry Mts., Slovak Republic). Neu Jb Mineral, Abh 185: 117–130

Putz H, PaarWH, Topa D, Horner J, Lüders V (2003) Structurally controlled gold and sulfosalt mineralization: the Altenberg example, Salzburg Province, Austria. Mineral Petrol 78: 111–138

Seifert T, Sandmann D (2006) Mineralogy and geochemistry of indium-bearing polymetallic vein-type deposits: implications for host minerals from the Freiberg district, Eastern Erzgebirge, Germany. Ore Geol Rev 28: 1–31

Sejkora J (2002) Mineral Association of the Burning Mine Dump of the Kateřina Mine at Radvanice near Trutnov, and Processes of Its Origin. Unpublished PhD thesis, Faculty of Science, Masaryk University, Brno, pp 1–144

Staude S, Dorn NA, Pfaff K, Markl G (2010) Assemblages of Ag–Bi sulfosalts and conditions of their formation: the type locality of schapbachite ($Ag_{0.4}Pb_{0.2}Bi_{0.4}S$) and neighboring mines in the Schwarzwald ore district, southern Germany. Canad Mineral 48: 441–466

Šrein V, Pažout R (2002) Contribution to the mineralogy of Kutná Hora ore district: Mn magnetite, Cr-muscovite, chromite. Bull mineral-petrolog Odd Nár Muz (Praha), 10: 290–293 (in Czech)

Topa D, Makovicky E (2010) The crystal chemistry of cosalite based on new electron-microprobe data and single-crystal determination of the structure. Canad Mineral 48: 1081–1107

Topa D, Makovicky E, Paar WH (2002) Composition ranges and exsolution pairs for the members of the bismuthinite–aikinite series from Felbertal, Austria. Canad Mineral 40: 849–869

Topa D, Makovicky E, Paar WH, Stanley CJ, Roberts AC (2011) Oscarkempffite, IMA 2011-029. CNMNC Newsletter No. 10: 2555

Topa D, Makovicky E, Paar WH (2013) Clino-oscarkempffite, IMA 2012-086. CNMNC Newsletter No. 16, Mineral Mag 77**:** 2695-2709

Voudouris PC, Spry PG, Mavrogonatos C, Sakellaris GA, Bristol SK, Melfos V, Fornadel AP (2013) Bismuthinite derivates, lillianite homologues, and bismuth sulfotellurides as indicators of gold mineralization in the Stanos shear-zone related deposit, Chalkidiki, northern Greece. Canad Mineral 51: 119–142

Wagner T, Cook NJ (1996) Bismuth–antimony sulfosalts from siderite-hosted vein mineralization, Apollo mine, Siegerland, FRG. Neu Jb Mineral, Abh 171: 135–153

Wagner T, Cook NJ (1997) Mineral reactions in sulphide systems as indicators of evolving fluid geochemistry – a case study from the Apollo mine, Siegerland, FRG. Mineral Mag 61: 573–590

Walenta K, Bernhardt H-J, Theye T (2004) Cubic $AgBiS_2$ (schapbachite) from the Silberbrünnle mine near Gengenbach in the Central Black Forest, Germany. Neu Jb Mineral, Mh 2004: 425–432

Wang N (1999) An experimental study of some solid solution in the system Ag_2S–PbS–Bi_2S_3 at low temperatures. Neu Jb Mineral, Mh 1999: 223–240

Yang H, Downs RT, Evans SH, Pinch W W (2013) Terrywallaceite, $AgPb(Sb,Bi)_3S_6$, isotypic with gustavite, a new mineral from Mina Herminia, Julcani Mining District, Huancavelica, Peru. Amer Miner 98: 1310–1314

Zakrzewski MA, Makovicky E (1986) Izoklakeite from Vena, Sweden, and the kobellite homologous series. Canad Mineral 24: 7–18

Zhang L, Wen H, Qin Ch, Du S, Zhu Ch, Fan H, Zhang J (2015) The geological significance of Pb–Bi- and Pb–Sb-sulphosalts in the Damajianshan tungsten polymetallic deposit, Yunnan Province, China. Ore Geol Rev 71: 203–214

Žák K, Sztacho P, Hušpauer M, Mikuš M (1993) Sulfide mineralization of the Kutná Hora ore district, Bohemian Massif, Czech Republic: stable isotope and fluid inclusion study. In: Final Meeting IGCP project No. 291 "Metamorphic Fluids and Ore Deposits". Abstracts, Prague, pp 68

Živkovič Ž, Živkovič D (1996) Comparative determination of the infinite dilution constants and interaction parameters in the binary system Bi–Sb. Rud Metalur Zbor 43: 215–218